Neuron, Vol. 19, 1187–1199, December, 1997, Copyright ©1997 by Cell Press

CLIP-115, a Novel Brain-Specific Cytoplasmic Linker Protein, Mediates the Localization of Dendritic Lamellar Bodies

Chris I. De Zeeuw,*§‖ Casper C. Hoogenraad,†§ Erika Goedknegt,* Elliot Hertzberg,‡ Andrea Neubauer,† Frank Grosveld,† and Niels Galjart†‖
*Department of Anatomy
†Department of Cell Biology
Erasmus University Rotterdam
P. O. Box 1738
3000 DR Rotterdam
The Netherlands
‡Department of Neuroscience
Albert Einstein College of Medicine
New York, New York 10461

Summary

Intracellular localization of organelles may depend in part on specific cytoplasmic linker proteins (CLIPs) that link membranous organelles to microtubules. Here, we characterize rat cDNAs encoding a novel, brain-specific CLIP of 115 kDa. This protein contains two N-terminal microtubule-binding domains and a long coiled-coil region; it binds to microtubules and is homologous to CLIP-170, a protein mediating the binding of endosomes to microtubules. CLIP-115 is enriched in the dendritic lamellar body (DLB), a recently discovered organelle predominantly present in bulbous dendritic appendages of neurons linked by dendrodendritic gap junctions. Local microtubule depolymerization leads to a temporary reduction of DLBs. These results suggest that CLIP-115 operates in the control of brain-specific organelle translocations.

Introduction

Microtubules are components of the cytoskeleton of eukaryotic cells that play an important role, for example, in the establishment of cell polarity (Wade and Hyman, 1997). Neurons are the most obvious example of a polarized cell type, with a myriad of dendrites that receive signals from the environment and their axon that can extend long distances. This polarized cell structure, which is not static but continuously subjected to plastic changes, requires neuronal microtubules to form an intraneuronal framework under precise temporal and spatial control. The adjustment of the microtubule cytoskeleton is partly mediated by microtubule-associated proteins (MAPs), which have been shown to determine the rate of growth of the microtubules by stabilizing their polymerization (Maccioni and Cambiazo, 1995). In neurons, MAP2 and tau are the dendrite- and axon-enriched prototypes of MAP, respectively (Craig and Banker, 1994). This differential distribution is in line with the different orientation patterns of the microtubules in dendrites and axons; axons have their microtubules organized with their plus ends pointed away from the cell body, while dendrites have microtubules oriented in both directions (Sharp et al., 1995; Schnapp, 1997).

Several lines of evidence indicate that microtubules also provide tracks for efficient organelle translocations and that they are essential for the general organization of membrane structures in a cell. For example, the endoplasmic reticulum forms a reticular network that colocalizes with microtubules, and the Golgi apparatus clusters around the region of the microtubule-organizing center (Cole and Lippincott-Schwartz, 1995). In addition, it has been demonstrated that depolymerization of microtubules, induced by application of nocodazole, can affect not only the movements and localization of membranous organelles but also their formation (Matteoni and Kreis, 1987; Cole et al., 1996).

The transport of organelles along microtubules is mediated by microtubule-based motor proteins, which serve as the engines of the translocation (Hirokawa, 1996; Vallee and Sheetz, 1996). Motor proteins are categorized according to the direction of the membrane movement that they carry out with respect to the plus and minus ends of microtubules. In general, plus end–directed transport is catalyzed by kinesins, while minus end–directed transport is catalyzed by cytoplasmic dynein (Hirokawa, 1996; Ogawa and Mohri, 1996). Recent characterization of ten kinesin superfamily proteins (KIFs) suggests that each member can, apart from some redundancy, convey a specific organelle or cargo. For example, KIFC2 has been reported to be a neuron-specific kinesin superfamily motor for dendritic transport of multivesicular body–like organelles (Saito et al., 1997; cf. Hanlon et al., 1997).

In the process of membrane trafficking, the motor proteins presumably interact with accessory factors that are required to guide each individual organelle to the appropriate motor protein. For example, kinectin has been identified as a putative kinesin receptor on membranes (Toyoshima et al., 1992; Burkhardt, 1996), and the dynactin complex is essential for the activity of dynein (Allan, 1996). One of the proteins of the dynactin complex is $p150^{glued}$ (Swaroop et al., 1987); it is supposed to link cytoplasmic dynein to its membranous cargo through interactions with a number of other components. This protein is a member of a novel family of microtubule-binding proteins, which is characterized by an N-terminal globular region with a novel type of microtubule-binding domain (MTB domain) and by a large coiled-coil region for protein–protein interactions (Vaughan and Vallee, 1995). Another member of this family is CLIP-170 (Pierre et al., 1992). This protein with an apparent M_r of 170 kDa has two MTB domains similar to the one of $p150^{glued}$, in addition to a long coiled-coil region. It was referred to as a cytoplasmic linker protein (CLIP) because it was shown to link endocytotic carrier vesicles to microtubules. On the basis of these findings, it was proposed that other CLIPs exist that could mediate the interaction of specific cytoplasmic organelles with microtubules (Rickard and Kreis, 1996).

Recently, a new membranous organelle, the dendritic

§ These authors contributed equally to this work.
‖ To whom correspondence should be addressed.

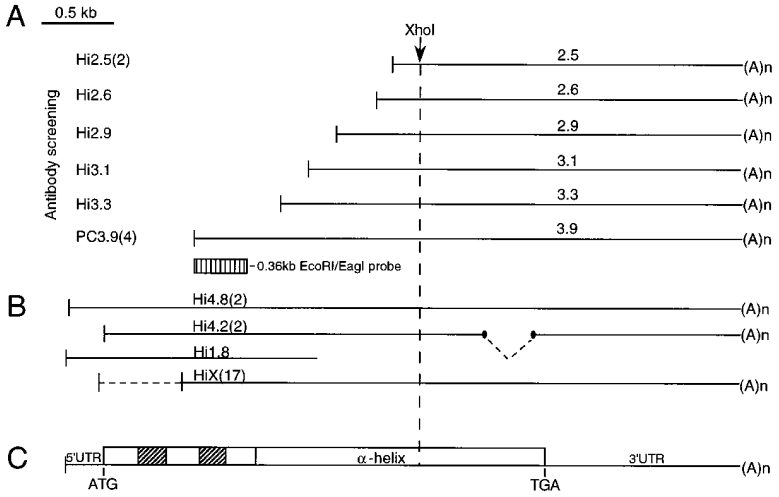

Figure 1. Cloning Strategy of *CLIP-115* cDNAs

(A) Ten cDNA clones isolated with antiserum α12B/18 from expression libraries of the hippocampus (Hi2.5, Hi2.6, Hi2.9, Hi3.1, Hi3.3) and piriform cortex (PC3.9). Clone Hi2.5 and clone PC3.9 were independently isolated two and four times, respectively.

(B) Twenty-two cDNA clones isolated from the hippocampus library with the use of a 0.36 kb EcoRI/EagI probe (striped box) from PC3.9; two nonidentical clones (Hi4.8) have an open reading frame that is preceded by an in-frame stop codon, while two other nonidentical clones (Hi4.2) miss 378 bp, presumably due to alternative splicing (stippled line).

(C) Structure of the composite 4.8 kb mRNA, including its 5′ and 3′ UTRs and the encoded novel protein product. The striped boxes within the open reading frame indicate the position of two repeated motifs within the protein.

lamellar body (DLB), was discovered (De Zeeuw et al., 1995). It occurs exclusively in bulbous dendritic appendages of neurons in particular brain regions such as the inferior olive, hippocampus, piriform cortex, and olfactory bulb. The function of DLBs remains to be elucidated, but several observations suggest it is related to that of dendrodendritic gap junctions, which are membrane specializations mediating electrotonic coupling between neurons. For example, during development, DLBs and dendrodendritic gap junctions arise simultaneously, while during adulthood, DLBs are present in all brain areas where gap junctions between dendrites of neurons are prominent. Moreover, the densities of both DLBs and dendrodendritic gap junctions in the inferior olive can be down-regulated concomitantly by removal of the cerebellar GABAergic afferents to electrotonically coupled olivary dendrites (De Zeeuw et al., 1997). In addition, the density of DLBs in olivary subnuclei can be correlated to the level of synchronous firing of these neurons. DLBs were discovered because they can be specifically labeled by batch #18 of antiserum α12B (α12B/18), which is an antiserum originally raised against a peptide (α12B) of the extracellular loop of gap junction protein connexin 43 (cx43) (De Zeeuw et al., 1995). Although this initially suggested the presence of cx43 in DLBs, we noted that DLB labeling is only observed with α12B/18, not with earlier batches of the antiserum or with other antibodies against cx43. Also, antiserum α12B/18, preabsorbed with matrix-linked peptide α12B, provides the same DLB immunoreactivity as nonpreabsorbed antiserum, and the affinity-purified antibody of α12B/18, eluted from the peptide α12B column, does not give DLB labeling. Therefore, we concluded that an antibody population is present in antiserum α12B/18 that is not directed against cx43 but against an unknown antigen component of DLBs (De Zeeuw et al., 1995).

In the present study, we used antiserum α12B/18 to isolate cDNAs encoding the DLB-specific antigen by expression screening of cDNA libraries of the brain areas with a high density of DLBs. All cDNAs are derived from the same mRNA and encode a novel, brain-specific protein, which is named CLIP-115 because of its strong similarity with CLIP-170 and its M_r of 115 kDa. Like its larger relative, CLIP-115 contains two MTB domains and a long coiled-coil region. Newly raised antibodies against CLIP-115 immunoreact with microtubules and DLBs. Depolymerization of the microtubules of neurons in the inferior olive by local application of nocodazole dramatically reduces the density of DLBs. We conclude that CLIP-115 is a protein constituent of DLBs, and we hypothesize that it determines the stucture and precise cytoplasmic location of DLBs. CLIP-115 and CLIP-170 may define a novel subfamily of proteins designed for the interaction of specific membranous organelles with microtubules.

Results

Expression Cloning of a Novel, Brain-Specific Cytoplasmic Linker Protein, CLIP-115

To isolate the α12B/18 antigen expressed in DLBs, λZAP expression libraries were made of areas with high densities of DLBs. A first screen of amplified hippocampus and piriform cortex cDNA libraries with antiserum α12B/18 resulted in the isolation of 68 positives. Secondary screening led to the positive identification of 10 clones, some of which are duplicates (Figure 1A). All clones were subsequently shown to have overlapping restriction enzyme maps and cross hybridizing inserts (data not shown). Six clones were characterized in detail, five from the hippocampus library with insert sizes of 2.5–3.3 kb (Hi2.5–3.3) and one clone from the piriform cortex library with an insert of 3.9 kb (PC3.9). Sequence analysis demonstrated that all clones come from the same transcript, suggesting that the antigenic determinant present in these clones reacts specifically with α12B/18. Since the 5′ end of the novel mRNA is not present in any of the clones, another screen of the hippocampus library was performed using a 0.36 kb DNA fragment as a probe; the fragment was subcloned from the 5′ end of PC3.9 (see Figure 1A). In this hybridization, 40 independent clones were isolated; 18 were later shown to encode rat CLIP-170, while 22 were 5′ end extensions of the clones isolated with α12B/18. Two of the latter have inserts of 4.8 kb (clones Hi4.8, Figure

1B). Hi1.8 starts more upstream than the two Hi4.8 fragments; the extra 50 bp sequence in the 5′ end of clone Hi1.8 is included in Figure 2. Two clones (Hi4.2) lack an internal fragment of 378 bp, presumably because of alternative splicing of primary transcripts. The structure and sequence of the composite 4.85 kb mRNA and the predicted secondary structure of the largest open reading frame (ORF) within the transcript are shown in Figures 1C and 2. The cDNA consists of a 5′ untranslated region (5′ UTR) of 288 nt, with a stop codon 42 bp upstream of and in-frame with the ATG that forms the translation start of a large ORF of 3141 bp. Deletion of the internal fragment of 378 bp from this ORF results in the removal of 126 amino acids from the predicted C-terminal end of the protein product, but the reading frame is maintained. A 3′ UTR of 1.3 kb follows the ORF. It contains two polyadenylation sites upstream of a poly(A)$^+$ tract (Figure 2). Translation of the ORF results in a protein of 1046 amino acids with a predicted molecular mass of 115 kDa. Its secondary structure suggests the presence of a globular N-terminal domain, which contains a doubly repeated motif of 69 amino acids and has runs of serine residues. Numerous sites for posttranslational modifications, such as casein kinase II–dependent phosphorylation, are scattered throughout the N-terminal domain. The N-terminal region also contains a small hydrophobic segment, which is located at amino acids 306–333 and which might form a transmembrane domain (Hofmann and Stoffel, 1993). It is followed by a large α-helical region of 699 amino acids, which contains stretches of heptad repeats. This domain is predicted to form a coiled-coil structure (Lupas, 1996).

Comparison of the amino acid sequence presented in Figure 2 to DNA/protein databases revealed we have cloned a novel cDNA encoding a protein with a striking homology to CLIP-170 (Pierre et al., 1992). CLIP-170 is identical to a protein called restin except for a 35 amino acid insert (Bilbe et al., 1992). Our novel protein, which we named CLIP-115, also contains the extra sequence present in restin. The overall identity and similarity between CLIP-115 and CLIP-170/restin are 45% and 67%, respectively (Figure 3A). When only the N-terminal regions are compared, these numbers rise to 58% and 77%. Immediately downstream of the repeats, CLIP-115 and CLIP-170/restin remain quite similar, but as the long coiled-coil regions are reached, similarity drops considerably. Moreover, the rod domain of CLIP-115 is much shorter than that of CLIP-170/restin, and the putative metal binding structure at the C terminus of CLIP-170/restin is not present in CLIP-115.

The doubly repeated motif in the N-terminal domain of CLIP-115, described above, corresponds to the MTB domains in CLIP-170/restin (Pierre et al., 1992, 1994). These domains, which differ from the MTB domains in MAPs (Lewis et al., 1988), can also be found in various other proteins from different organisms; these include DP-150 (Holzbaur et al., 1991), p150^{glued} (Swaroop et al., 1987), BIK1 (Trueheart et al., 1987), CKAPI (Watanabe et al., 1996), Ssm4 (Yamashita et al., 1997), and kinesin-73 (Li et al., 1997). Rat DP-150 and its Drosophila melanogaster homolog p150^{glued} are part of the dynactin complex and are involved in dynein-dependent vesicle movements along microtubules (Gill et al., 1991). Kinesin-73 is a motor protein in Drosophila with an MTB domain located in the C-terminal region of the protein (Li et al., 1997). BIK1, a 60 kDa protein from Saccharomyces cerevisiae, is required for microtubule-related functions during mitosis (Berlin et al., 1990), while Ssm4 is a protein that modifies the structure and/or function of nuclear microtubules in order to promote meiotic nuclear division (Yamashita et al., 1997). In addition, approximately 60 mammalian expressed sequence tags (ESTs) with this novel domain can be found in the databases. Thus, the type of motif present twice in the N-terminal domain of CLIP-115 and CLIP-170 occurs as a single domain in numerous proteins involved in a variety of intracellular processes and is highly conserved throughout evolution. It is noteworthy, however, that the number of proteins with such a presumptive MTB domain has expanded particularly in mammals.

Alignment of the motifs in the N-terminal domain of CLIP-115 to those of CLIP-170/restin and other proteins with homologous domains (Figure 3B) allows us to extend the size of the consensus MTB domain in comparison to previous reports (e.g., Pierre et al., 1992; Watanabe et al., 1996). This extension appears valid because glycine and valine, which are characteristic amino acid residues in the consensus motif, are also present at the boundaries of the extended domain. The alignment emphasizes two other points. First, it shows that the CLIP-115 repeats best resemble those of CLIP-170/restin. The identity between the first MTB domain of CLIP-115 and CLIP-170/restin is 78% (similarity 93%), while for the second MTB domain, this number equals 86% (similarity 97%). These data strongly suggest that CLIP-115 indeed also binds to microtubules. Second, CLIP-115 and CLIP-170/restin are so far the only proteins with two MTB domains instead of one. This observation emphasizes the high degree of similarity between these proteins and suggests a specific function might be assigned to CLIP-115 and CLIP-170.

Northern blot analysis of rat and mouse tissues, using rat *CLIP-115* cDNA fragments as probes, revealed the presence in both organisms of transcripts of $\sim$5 kb (Figure 4). Thus, the rat *CLIP-115* cDNA sequence, depicted in Figure 2, is probably full-length, and rat and mouse mRNAs must be highly homologous. In the adult rat, mRNA is detected not only in areas like the hippocampus, inferior olive, and piriform cortex, where DLBs are prominent, but also in the cerebellum, where DLBs have not been shown to occur (Figure 4A) (De Zeeuw et al., 1995). In the adult mouse, *CLIP-115* mRNA is detected in the brain but not in testis, thymus, liver, spleen, and heart. *CLIP-115* is present at very low doses in kidney, and a weakly hybridizing band of $\sim$6–7 kb is also detected in lung; *CLIP-115* thus appears to be quite specific for neurons and/or glia cells. No difference in expression level is seen between male and female adult brain. During development, expression of *CLIP-115* oscillates (Figure 4B). Message is undetectable in embryonic stem cells, but at E10.5, the first embryonic time point tested, transcript is readily detected. As development proceeds, message levels appear to decline until birth, after which *CLIP-115* mRNA suddenly increases. Subsequently, the message gradually decreases until postnatal day 10, the day when DLBs start to occur (De

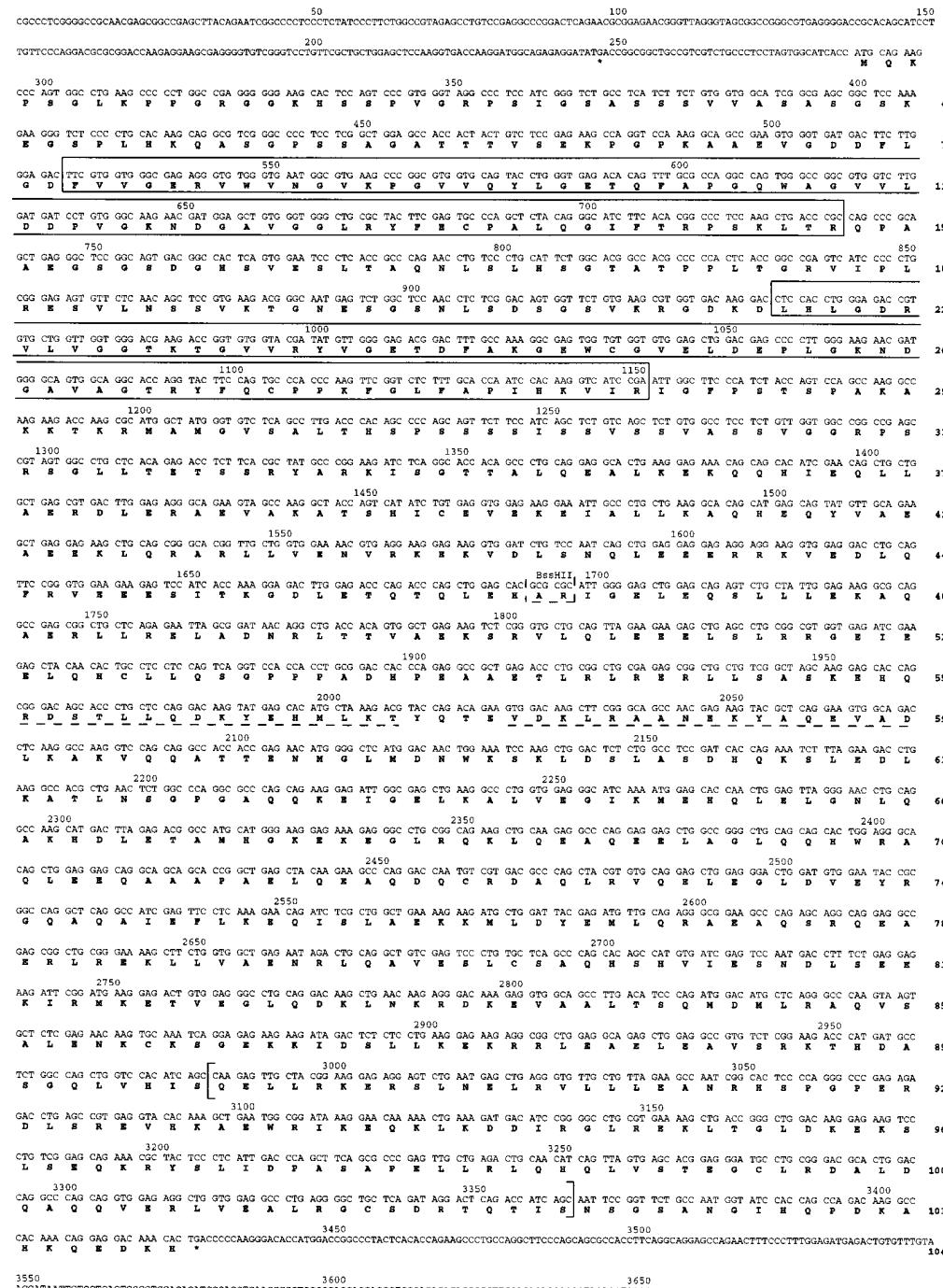

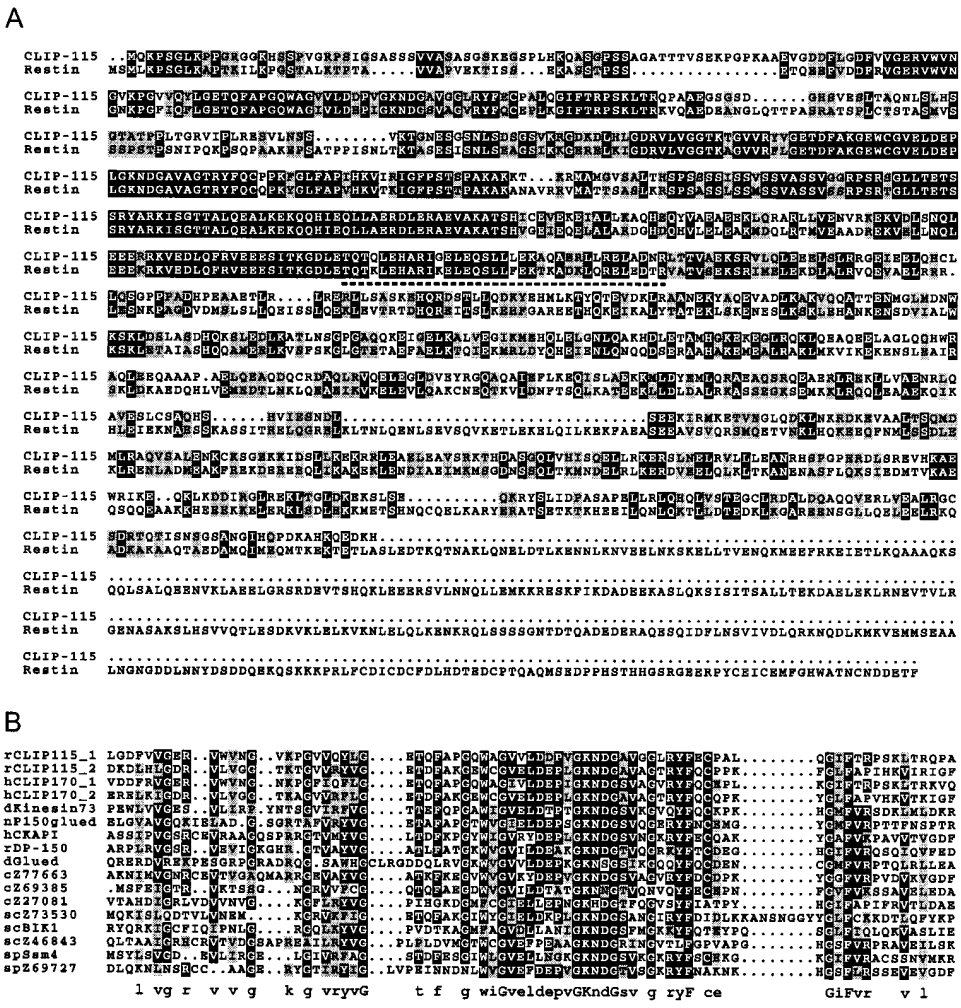

Figure 3. CLIP-115 and Its Similarity to Other Proteins

(A) Alignment of rat CLIP-115 with restin, which is identical to human CLIP-170 except for an additional 35 amino acids (dashed line). Note the very high degree of similarity in the N-terminal regions of CLIP-115 and CLIP-170/restin.

(B) Alignment of the MTB domains of CLIP-115 with those of other fully sequenced proteins, i.e., h(uman) CLIP-170, r(at) 150k DAP, d(rosophila) Glued, n(eurospora) p150 Glued, h CKAPI, S(accharomyces) c(erevisiae) BIK1, S(accharomyces) p(ombe) Ssm4, and the yeast (sc/sp) and C. elegans (c) hypothetical proteins with accession numbers Z73530, Z46843, Z69727, Z77663, Z69385, and Z27081. Sequences were taken from the SwissProt database and aligned using ClustalW and GCG software packages. Black boxes indicate that more than 50% of the aligned sequence contains a particular amino acid, while conserved amino acid substitutions are represented by a gray outline. The consensus sequence for the MTB domain is given below the alignment: capital letters indicate complete conservation, while small letters indicate a preference for a particular residue.

Zeeuw et al., 1995). At that point, the message increases again and reaches the levels present in adult brain. Thus, the variation in *CLIP-115* mRNA levels seems to reflect a differential need for the protein during mouse development.

In conclusion, using antiserum α12B/18, we have cloned cDNAs, which encode a protein with homology to CLIP-170/restin. The similarity is most prominent in two MTB domains, suggesting that the novel protein CLIP-115 can bind to microtubules. The fact that all cDNAs from the two expression libraries are derived from a single, brain-specific message strongly suggests that we cloned the DLB-specific antigen detected by α12B/18. However, *CLIP-115* mRNA is present in the

Figure 2. Nucleotide and Deduced Amino Acid Sequence of *CLIP-115* cDNAs

Sequence of the composite cDNA depicted in Figure 1C. Nucleotide numbering is shown above the sequence, while amino acid numbering is indicated in the right margin. The plain boxed sequences indicate the MTB domains; the BssHII site is indicated to show how the CLIP-$115_{1–468}$ sequence for the GFP experiments in Figure 5 was generated; dashed lines underscore the 16 or 17 amino acid peptides (dIb-2 and dIb-1, respectively) that were used for raising antibodies. Asterisks denote stop codons; brackets indicate the region of presumed alternative splicing; the dashed boxes indicate polyadenylation sites.

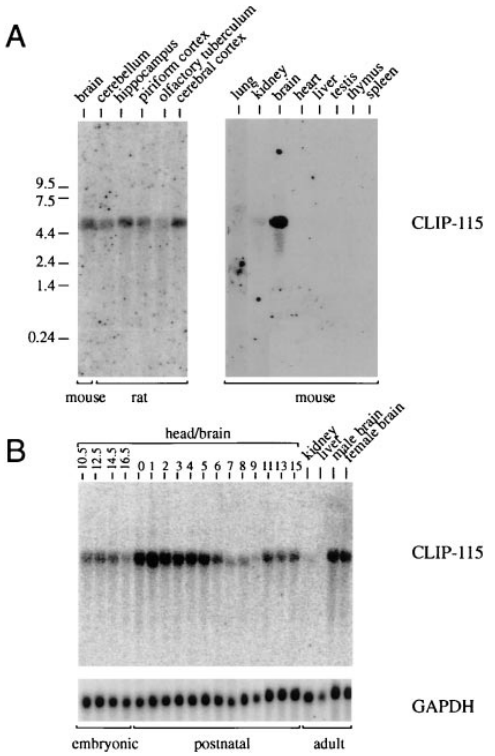

Figure 4. Expression of *CLIP-115* mRNA

(A) Northern blots, containing ~15 μg of total RNA from different tissues, were screened with *CLIP-115*–specific DNA probes.

(B) Comparable amounts of total mouse RNA, isolated from embryonic or postnatal heads/brains at the indicated time points during development, were screened for *CLIP-115* message as in (A). To control for RNA quantity, the developmental blot was reprobed with a cDNA encoding the glycolytic enzyme GAPDH. The variation in *CLIP-115* mRNA level was normalized to that of GAPDH with phosphorimage analysis.

cerebellum, while DLBs are not, and *CLIP-115* mRNA occurs during development before the final formation of DLBs. Thus, we set out experiments to determine whether CLIP-115 can indeed bind to microtubules and to find out whether it is a protein constituent of DLBs.

Localization of CLIP-115 In Vitro

To characterize CLIP-115 at the protein level, different antibodies were raised against peptides derived from the unique coiled-coil domain of the protein (antisera #2131 and #2133; see Figure 2) or against the MTB domain (α-MTCLIP115). The specificity of the new antisera against CLIP-115 was tested on Western blot and in fluorescence experiments. COS1 cells were transfected with normal, full-length CLIP-115, with a protein lacking the alternatively spliced sequence (δCLIP-115), or with CLIP-115 linked to green fluorescent protein (GFP-CLIP-115). As a control, mock transfected cells were included. Two days after transfection, cells were harvested and total protein extracts were made. Proteins were run alone or next to total protein homogenates from mouse kidney, liver, and brain, Western blotted, and incubated with antibodies against GFP and MTCLIP115 (Figure 5A) or affinity-purified #2133 antibodies (Figure 5B). The experiments demonstrate that CLIP-115, δCLIP-115, and GFP-CLIP-115 are produced in the COS1 cells as proteins of the expected size. Each protein is subjected to partial proteolytic degradation; this is particularly evident with the α-GFP antibody. The anti-MTCLIP115 antibodies recognize each CLIP variant, but in addition, other common proteins are detected. Therefore, we used affinity-purified anti-peptide antibodies against a unique stretch of the coiled-coil region of CLIP-115 to detect the protein in vivo (Figure 5B). This antiserum recognizes two proteins of approximately 110–140 kDa specifically in brain tissue, which is consistent with the Northern blot expression results. In addition, the anti-peptide antibodies recognize CLIP-115 in transfected COS1 cells. The mouse proteins comigrate with the rat-derived CLIP-115 isoforms produced in COS1 cells, suggesting that the sizes of the two isoforms of CLIP-115 produced in mouse brain are similar to those of the rat and that the antibodies are specific for CLIP-115.

In the fluorescence experiments, both transfected COS1 cells (Figures 5C–5J) and cultured neurons from the hippocampus (Figures 5K and 5L) were investigated. In the COS1 cells transfected with the CLIP-115 isoforms, a clear fluorescent labeling pattern, which appears as long centrifugal fine wires in the cytoplasm, can be observed with both antisera #2131 (data not shown) and #2133 (Figure 5E); no immunolabeling is detected in nontransfected cells (Figures 5C and 5D). The labeling pattern of CLIP-115 revealed with antiserum #2133 completely overlaps with that obtained with anti-β-tubulin antibodies (Figure 5F). From these data, we conclude that CLIP-115, overexpressed in COS1 cells, colocalizes with the microtubule cytoskeleton.

This association was further confirmed by experiments in which COS1 cells were transfected with GFP-CLIP-115, GFP-δCLIP-115, or GFP linked to a truncated N-terminal mutant spanning amino acid residues 1–468 (GFP-$CLIP_{1–468}$). GFP-CLIP-115 fluorescent labeling in transfected COS1 cells is still very strong after mild fixation with paraformaldehyde, and it is virtually identical to that obtained with antisera #2131 and #2133 in CLIP-115–transfected cells (compare Figures 5E and 5G). This finding emphasizes the specificity of the new antisera against CLIP-115. The labeling extends into the long and thin outgrowths of the COS1 cells when these are present (data not shown). When GFP-$CLIP_{1–468}$ is used, the labeling of the cytoplasmic microtubules of the COS1 cells intensifies, and the microtubules appear to be clustered in thick bundles (for comparison with distribution of β-tubulin, see Figures 5I and 5J). Thus, expression of the MTB domains of CLIP-115 without the large coiled-coil region leads to enhanced bundling of the cytoskeletal microtubule network. This phenomenon has been observed previously in experiments using CLIP-170 or $p150^{glued}$ deletion constructs and could be due to cross-linking of the microtubules (Pierre et al., 1994; Waterman-Storer et al., 1995).

Finally, to demonstrate that CLIP-115 is also associated with microtubules in neurons, we investigated the distributions of CLIP-115 and MAP2 in a monolayer of differentiating cultured neurons from the hippocampus. As shown in Figures 5K and 5L, CLIP-115 colocalizes with MAP2 in all (i.e., both proximal and distal) dendritic

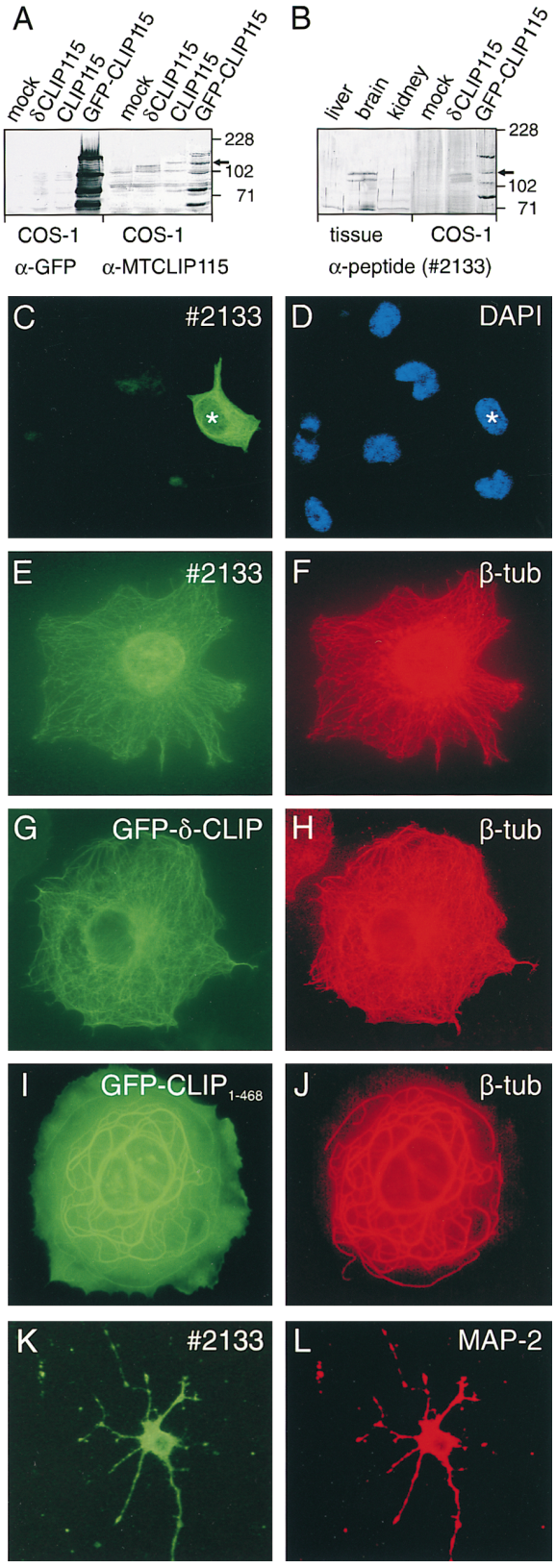

Figure 5. CLIP-115 Expression in Tissue Extracts, COS1 Cells, and Cultured Neurons

(A and B) CLIP-115 expression analyzed on Western blot. In (A), protein extracts from mock transfected COS1 cells or from cells transfected with CLIP-115, δCLIP-115, and GFP-CLIP-115 were run on gel, blotted, and incubated with α-GFP or α-MTCLIP115 antibodies. CLIP-115, δCLIP-115, and GFP-CLIP-115 proteins of the correct size are produced. The arrow indicates full-length CLIP-115 in the GFP-CLIP115 lane incubated with α-MTCLIP115 antibodies; proteolytic processing leads to the appearance of this protein, as it is not recognized by α-GFP. In (B), protein extracts from mouse brain, liver, and kidney as well as COS1 cells were tested for the presence of CLIP-115 with the use of affinity-purified #2133. The arrow points at the position of presumptive CLIP-115 generated by proteolytic processing in the GFP-CLIP115 lane.

(C–J) Fluorescence study of CLIP-115 expression in COS1 cells. In (C) and (E), the pattern of CLIP-115 as detected with antiserum #2133 consists of a centrifugal fine wire network in the cytoplasm. In (C), one transfected cell (asterisk) is surrounded by nontransfected cells that are identified by DAPI staining of their nuclei in (D). (F) The CLIP labeling pattern colocalizes with the microtubule network as revealed by β-tubulin labeling. CLIP-115 expression was also investigated in COS1 cells transfected with constructs expressing GFP, linked to δCLIP-115 (G) and $CLIP_{1-468}$ (I). Note that the labeling pattern obtained in (G) is virtually identical to that in (E). (I) Expression of mutant GFP-$CLIP_{1-468}$ causes thickening of the microtubule bundles. GFP signals colocalize with anti-β-tubulin staining pattern in both (H) and (J).

(K and L) CLIP-115 expression in cultured neurons. CLIP-115 (K) is expressed in all the dendritic components of differentiating hippocampal neurons that contain the microtubule-associated protein MAP2 (L).

components of these neurons. Taken together, these experiments suggest that (1) CLIP-115 indeed binds to microtubules; (2) the microtubule-binding property of CLIP-115 is mediated by the two MTB domains in its N-terminal region; and (3) the peptide antisera against CLIP-115 are specific and can be further employed on tissue sections.

Localization of CLIP-115 In Vivo

To determine whether CLIP-115 is located in DLBs, the newly raised antisera #2131 and #2133 were used for immunocytochemistry on adult rat brain sections. Both light microscopic and electron microscopic analyses were carried out (Figures 6 and 7). In general, both antisera revealed the same labeling pattern in the three areas of the brain with the highest density of DLBs, i.e., the inferior olive, hippocampus, and piriform cortex. Since these antisera are raised against different regions of CLIP-115, this suggests that the labeling seen is specific for CLIP-115. In the light microscopic analysis, we observed that in the inferior olive, the most prominent labeling is, apart from some weak cytoplasmic dendritic staining, an overall punctate labeling ubiquitously distributed in the neuropil of all its subnuclei (Figures 6A and 6C; for comparison with labeling obtained with antiserum α12B/18, see Figure 8B); this labeling is abolished by preincubation of the antisera with bacterially produced GST-CLIP115 (Figure 6B), strongly suggesting the antibodies specifically recognize CLIP-115. In the hippocampus and piriform cortex, the most prominent staining is found in the dendrites of the pyramidal cells (Figure 6D), while modest punctate labeling can be seen in the neuropil. In the cerebellum, we observed a specific labeling of the fiber extensions of all Bergmann glia cells in the molecular layer of the cerebellar cortex (Figures 6E and 6F). The proximal parts of the cytoplasm of the

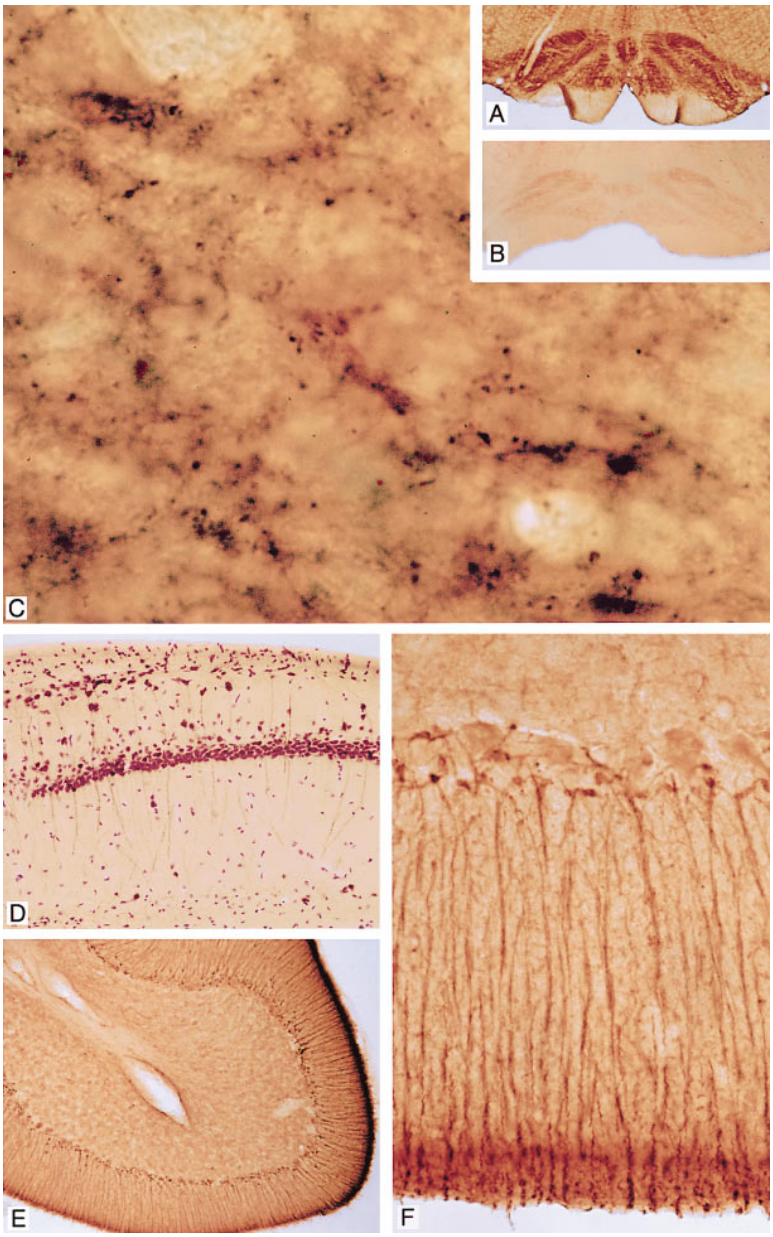

Figure 6. Distribution of CLIP-115 in the Rat Brain

Labeling patterns of CLIP-115 obtained with antiserum #2131 and #2133.

(A) Labeling in the ventral medulla oblongata. Note the ubiquitous immunolabeling in all subnuclei of the inferior olive.

(B) Labeling of the same structure with antiserum #2133 preabsorbed with bacterially produced CLIP-115.

(C) High magnification of the rostral medial accessory olive, the olivary subnucleus with the highest density of immunoreactive puncta.

(D) Labeled dendrites of pyramidal cells in the CA1 area of the hippocampus. This micrograph was taken from a section counterstained with cresyl violet.

(E) Labeled Bergmann glia fibers in the molecular layer of the cerebellar cortex.

(F) Same fibers at a higher magnification; note that the cell bodies of the Bergmann glia cells are not labeled, whereas the proximal parts of the fibers are densely stained. The labeled fibers extend into the extreme outer part of the molecular layer.

Bergmann fibers are more prominently labeled than the peripheral parts. The cell bodies of the Bergmann glia cells are not labeled. Identical results were obtained with affinity-purified #2133 antiserum both on rat and mouse brain sections (data not shown), again suggesting that the labeling with the peptide antisera on brain sections is specific for CLIP-115.

In the electron microscopic analysis, we found that the punctate labeling in the inferior olive corresponds to DLBs (Figure 7); the morphology of the DLBs, as revealed with the new antisera against CLIP-115, is the same as that of the DLBs labeled with antiserum α12B/18 (compare Figures 7B and 7D). The preimmune sera of #2131 and #2133 as well as antisera against CLIP-170 (Pierre et al., 1992, 1994) do not label DLBs. Within DLBs, the most abundant labeling occurs in the electron dense depositis in between the lamellar stacks, which are approximately 60 nm apart from one another. Most of the cytoplasmic labeling in dendrites of olivary neurons, on the other hand, corresponds to clusters of microtubules (for labeling with antiserum #2133, see Figures 7C and 7E; with antiserum #2131, see Figure 7F). Apparently, antisera #2131 and #2133 do not only detect microtubules in vitro, as described above for COS1 cells and cultured hippocampal neurons, but also in vivo. The dendrites containing labeled microtubules belong to all possible categories, i.e., proximal, intermediate, and distal dendrites. Interestingly, the microtubules labeled with antisera #2131 or #2133 are frequently located in the vicinity of labeled vesicles, while the nonlabeled microtubules within the same dendritic profile are not associated with vesicles (e.g., Figure 7C). Therefore, it appears possible that CLIP-115 establishes a link between microtubules and membranous vesicles.

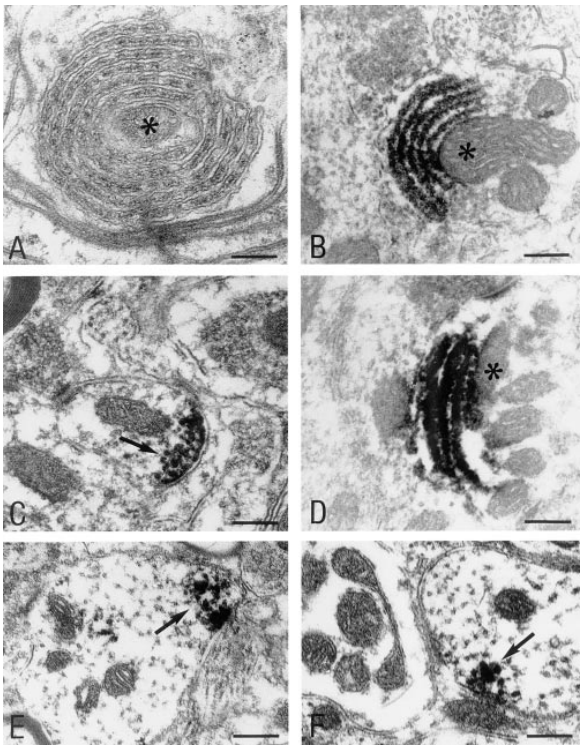

Figure 7. CLIP-115 Is Localized in DLBs and Microtubules

Detailed analysis of the punctate labeling in the inferior olive as presented in Figures 6A and B demonstrates that the dots and cytoplasmic dendritic labeling correspond to DLBs and clusters of microtubules, respectively.

(A) Shows the characteristic morphology of a DLB following standard electron microscopy. Note that the lamella are surrounding a mitochondrion (asterisk) located in the center of the organelle.

(B) Shows a DLB labeled with antiserum α12B/18 ([A] and [B] are modified from De Zeeuw et al., 1995).

(C) Shows a cluster of labeled microtubules in a distal dendrite following immunocytochemistry with antiserum #2133 against CLIP-115. Note that the labeled microtubules indicated by the arrow surround a labeled vesicle.

(D) Shows a DLB labeled with antiserum #2133; this DLB is highly similar to the DLB labeled by antiserum α12B/18 in (B).

(E and F) Show intermediate dendrites with clusters of microtubules labeled with the use of antisera #2133 and #2131, respectively. Scale bars in (A), (B), (C), (D), (E), and (F) indicate 26 μm, 26 μm, 0.25 μm, 0.27 μm, 31 μm, and 30 μm, respectively.

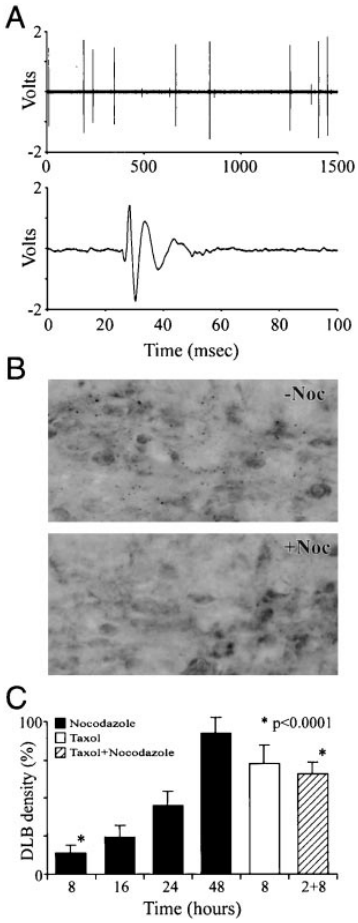

Figure 8. Microtubule Depolymerization In Vivo Affects the Density of DLBs

The density of DLBs in the inferior olive of the rat brainstem was investigated after several periods of survival time following local injection of nocodazole.

(A) Shows the electrophysiological identification of a neuron in the rat inferior olive. Olivary neurons can be recognized by their low firing frequency of 0.5–1 Hz (top) and by the characteristic wave shape of their action potential (bottom).

(B) Shows the effect of nocodazole on the density of DLBs in the rostral medial accessory olive of the rat 8 hrs after the injection. Note the reduction in immunoreactive puncta (revealed with antiserum α12B/18).

(C) Shows the densities of DLBs in the olive at different survival times following local application of nocodazole, taxol, or both drugs. Following nocodazole alone, the density of DLBs was reduced to 14%, 24%, 46%, and 94% of the normal density after 8, 16, 24, and 48 hrs of survival, respectively. Although taxol itself evoked a mild reducing effect on the density of DLBs, it practically abolished the reducing effect of nocodazole; when the inferior olive was injected with taxol 2 hrs prior to the nocodazole application, the density of DLBs 8 hrs after the nocodazole injection was reduced to 73% instead of 14%. This difference was significant ($p < 0.0001$; Wilcoxon rank-sum test).

These vesicles in turn, then, might be specifically involved in the formation or turnover of the DLBs.

The Effect of Microtubule Depolymerization on the Density of DLBs

Above, it is shown that CLIP-115 can bind to microtubules and that DLBs are detected with antisera against CLIP-115. To find out whether and to what extent microtubules are necessary for the localization of DLBs in vivo, we investigated the effects of depolymerization of microtubules on the distribution of DLBs by local application of nocodazole and taxol (Kolodney and Elson, 1995). Eight and sixteen hours after unilateral extracellular application of nocodazole to the rat inferior olive (for electrophysiological identification, see Figure 8A), the density of olivary DLBs was reduced to 14% and 24% of normal values (Figures 8B and 8C) (for an overview of absolute densities of DLBs in different olivary subnuclei, see De Zeeuw et al., 1995). The number of Nissl-stained neurons in the inferior olive, quantified as a control, remained the same. Twenty-four and forty-eight hours after intraolivary injection of nocodazole,

the DLBs reappeared (46% and 94% of normal values, respectively). Injection of the carrier alone, i.e., 25% DMSO, did not result in reduction of DLBs. When the inferior olive was injected with the microtubule stabilizing drug taxol 2 hrs prior to nocodazole application, the density of DLBs 8 hrs after the nocodazole injections was reduced to 73% instead of 14% (Figure 8C). This difference strongly suggests that the DLB reducing effect of nocodazole is caused by depolymerization of the microtubules. These experiments indicate that the formation of DLBs, as detected by α12B/18, is dependent on the presence of normal polymerized microtubules, and they suggest there is a continuous and rapid turnover of DLBs in olivary neurons.

Discussion

Recently, we discovered a new neuronal organelle, the dendritic lamellar body (DLB), which is exclusively located in the bulbous appendages of dendrites of neurons with dendrodendritic gap junctions (De Zeeuw et al., 1995). This organelle can be specifically labeled with antiserum α12B/18, which was raised against one of the extracellular loops of the gap junction protein cx43. However, until now, it was not clear what epitope is detected by this antiserum. Here, we determined the identity of the epitope by producing cDNA libraries of brain areas with high densities of DLBs and screening these with α12B/18. We characterized ten clones from two different cDNA libraries, yet we showed that all clones are derived from the same mRNA. These data strongly suggest that the isolation of these clones is due to the presence of a specific antibody population in α12B/18 directed against the protein product encoded by the different cDNAs. This protein is brain-specific and is referred to as CLIP-115 because of its homology with CLIP-170. Newly raised antisera against CLIP-115 were found to label DLBs. Thus, we conclusively demonstrated that we have isolated the antigen in the α12B/18 antiserum that is specific for DLBs, and thereby we identified a novel protein component of this intriguing neuronal organelle. By using (parts of) CLIP-115 in yeast two-hybrid screens, other protein constituents of DLBs can now be isolated.

Previously, we showed that α12B/18 antibodies detect proteins in rat brain of 110–140 kDa on Western blots, which are present only in those areas of the brain that contain DLBs (De Zeeuw et al., 1995). The sizes calculated from those SDS-PAGE experiments correlate well with the predicted molecular mass of CLIP-115, and the fact that two proteins were detected on Western blots can be explained by assuming that specific post-translational modifications take place on CLIP-115 and/or that different brain areas express either one of the two alternative splice products of CLIP-115. Interestingly, two isoforms of CLIP-115 are also specifically detected in mouse brain, using anti-peptide antibodies against rat CLIP-115. The finding that CLIP-115 is detected in the cerebellum, in both rat and mouse and at both mRNA and protein level, whereas the DLB-specific antigen in α12B/18 is not, is probably due to the stringent conditions under which incubatons with α12B/18 were done. The same conditions were used for screening the cDNA libraries with α12B/18 and yielded only one type of clone. Thus, it is presumably the high local concentration of CLIP-115 in DLBs and recombinant CLIP in phage lysates that permits its clean detection by α12B/18 under stringent conditions, both in tissue sections and on nitrocellulose filters.

Within DLBs, most of the CLIP-115 labeling occurs in the electron-dense depositis between the lamellar stacks. This observation raises the possibility that CLIP-115 is not only necessary for the localization of DLBs in dendrites but also for the appropriate distance between the membraneous stacks within a DLB; this distance is approximately 60 nm and could correspond to the length of the coiled-coil domain in CLIP-115 (Moore and Endow, 1996). CLIP-115 would therefore have a role as a structural determinant of DLB morphology in addition to its more general function as a membrane–microtubule linking molecule. Because of the morphological resemblance between DLBs and calciosomes (Villa et al., 1991), we have tested whether CLIP-115 is expressed in calciosomes but found no evidence for the presence of the protein there. Interestingly, calciosomes have more closely packed membranous stacks than DLBs, a feature that may be due to the lack of CLIP-115 (or the presence of a shorter unknown CLIP). We have also attempted to label DLBs with markers for IP3 and ryanodine receptors, which are found on calciosomes (Takei et al., 1992), but none of these receptors was found to colocalize with DLBs (data not shown). In spite of these findings, DLBs might still operate as a special type of intracellular calcium storage site. This possibility is supported not only by their morphologic resemblance with calciosomes but also by the fact that dendritic calcium spikes have been identified in most, if not all, of the brain areas with DLBs (e.g., Llinás and Yarom, 1981; Andreasen and Nedergaard, 1996).

DLBs have been associated with dendrodendritic gap junctions because of their overlapping distribution in the brain and their simultaneous occurrence during development (De Zeeuw et al., 1995). In addition, DLBs and dendrodendritic gap junctions can be down-regulated concomitantly, and the level of electrotonic coupling of neurons can be correlated to the density of DLBs (De Zeeuw et al., 1997). Based upon these observations, we have proposed that DLBs are necessary for the turnover and/or assembly of dendrodendritic gap junction channels, which are usually being replaced in only a few hours (Laird et al., 1991). Since CLIP-115 is a structural component of DLBs in dendritic varicosities, and the turnover of DLBs following application of nocodazole is as rapid as that of gap junctions, it is possible that CLIP-115 is also involved in the maintenance of dendrodendritic gap junctions. In this respect, it is interesting to note that Bergmann glia cells, which do not contain DLBs but prominently express CLIP-115, are coupled by extremely extensive gap junction plaques (Palay and Chan-Palay, 1974). Moreover, CLIP-170 has also been associated with membrane specializations, i.e., desmosomal plaques (Wacker et al., 1992). Thus, both these observations are compatible with a proposed role of CLIP-115 in the formation and/or turnover of gap junctions.

The definition of cytoplasmic linker proteins implies their involvement in the translocation of cytoplasmic organelles as well as their proper intracellular localization. Similar to the hypothesis that each member of the kinesin superfamily of motor proteins conveys a specific organelle (Hirokawa, 1996; Saito et al., 1997), it has been proposed that for each type of membrane, a different CLIP might exist (Rickard and Kreis, 1996). However, whereas ten different members of the kinesin superfamily have already been identified (Hirokawa, 1996), CLIP-170, which links endocytotic vesicles to microtubules, is so far the only protein that has been identified as a cytoplasmic binding factor in vivo (Pierre et al., 1992). In the present study, we demonstrate that its close relative CLIP-115 is associated with the membranes of DLBs, that CLIP-115 contains MTB domains that function as such both in vitro and in vivo, and that depolymerization of microtubules by nocodazole application in vivo influences the (trans)location of DLBs. Thus, CLIP-115 indeed appears to mediate the interaction between microtubules and a highly specific neuronal organelle with a particular localization. It is noteworthy that of the large family of proteins with the novel MTB domain described to date, only CLIP-115 and −170 have a tandem motif and also are the only proteins that have been shown to associate directly with particular membranes and microtubules. Therefore, a repeated MTB domain might be characteristic for proteins directly interacting with membranous organelles and microtubules. By cloning CLIP-115 and determining its distribution, we lend support to the theory that multiple CLIPs exist and that they are involved in the localization of organelles (Rickard and Kreis, 1996), but it remains to be shown whether each type of membranous organelle has its own CLIP and to what extent each CLIP binds to specific organelles.

Experimental Procedures

cDNA Libraries

Brain regions highly enriched for hippocampus, piriform cortex, inferior olive, frontal cortex, cerebellum, and olfactory bulb were collected from 20 adult male Wistar rats, and total cellular RNA was extracted (Auffray and Rougeon, 1980). Five micrograms of poly(A)$^+$ mRNA was isolated from the three brain areas with the highest density of DLBs (i.e., hippocampus, piriform cortex, and inferior olive) with the use of magnetic oligo(dT)$_{25}$ Dynabeads (Dynal, Oslo, Norway). Double-stranded cDNAs were made, and fragments longer than 500 bp were force cloned into lambda ZAP Express (Stratagene). Libraries were packaged with Gigapack II Gold (Stratagene).

Cloning and Sequencing of *CLIP-115* cDNAs

The hippocampus and piriform cortex libraries (complexity of 1.1×10^6 and 0.7×10^6 independent clones, respectively) were plated and screened using antiserum α12B/18 (1:1000) according to standard procedures (Sambrook et al., 1989). Positive clones were plaque purified, and inserts were excised using the Rapid Excision kit (Stratagene). To obtain full-length cDNAs, the hippocampus library was replated and screened with a DNA probe, which was a labeled 0.36 kb EcoRI-EagI fragment from the 5′ end of clone PC3.9 (Figure 1A) (Feinberg and Vogelstein, 1983). The CLIP-115 nucleotide sequence was determined on both strands with ^{35}S-dATP and Sequenase (Amersham).

Northern Blot Analysis

Total RNA from mouse and rat tissues was isolated as described above. RNA samples were electrophoresed on a 0.8% agarose gel containing 0.66 M formaldehyde (Fourney et al., 1988), blotted onto Hybond N$^+$ nylon membranes (Amersham), and hybridized according to standard procedures (Sambrook et al., 1989) with different *CLIP-115* DNA probes, labeled as above. Filters were exposed to Phosphorimager screens and images acquired through Imagequant (Molecular Dynamics).

Generation of Antisera

Full-length CLIP-115 and the N-terminal region including the MTB domains (MTCLIP115) were fused to glutathione S-transferase (GST) using pGEX2T (Pharmacia). Both GST fusion proteins were induced in bacteria and purified (Smith et al., 1988). In addition, two peptides of 17 (dIb-1) or 16 (dIb-2) amino acids were synthesized, and 0.5 mg of each peptide was conjugated to 2 mg of thyroglobulin (Sigma) using 0.15% glutaraldehyde in phosphate buffer. Purified GST-MTCLIP-115 and the conjugated dialyzed peptides were injected into New Zealand White rabbits in a suspension of Freund's incomplete adjuvans. Serum from rabbit #2131 is against peptide dIb-1, and serum from #2133 is against peptide dIb-2 (see Figure 2). Serum #2133 was affinity purified on filter strips containing GST-CLIP-115. The unbound or depleted antibody population was used in the experiments shown in Figure 6B. The bound antibody pool was eluted from the filter using 0.1 M glycine (pH 2.3) and 1 M NaCl. After elution, the pH was quickly restored with unbuffered Tris. Affinity-purified antibodies were concentrated on centricon-30 membranes (Amicon) and stored in the presence of 0.1 mg/ml BSA.

Western Blot Analysis

Total protein extracts from COS1 cells were obtained 2 days after transfection. After sonication, cell lysates were boiled in SDS sample buffer in the presence of DTT. Mouse brain, liver, and kidney were homogenized in PBS in the presence of protease inhibitors (Boehringer Mannheim) and further treated as above. Equal amounts of protein homogenates were analyzed on 7% SDS-polyacrylamide gels and by Western blots (Sambrook et al., 1989). Blots were blocked for 1 hr in 10 mM Tris (pH 7.6), 100 mM NaCl, 0.05% Tween (TNT) containing 3 mg/ml BSA and incubated with α-GFP (Clontech; 1:4000), α-MTCLIP115 (1:1000), or affinity-purified #2133 (1:50) for 2 hrs at room temperature. After washing in TNT buffer, goat-anti rabbit antibody coupled to alkaline phosphatase (Sigma, 1:2000) was added to the blots in TNT/BSA buffer for 2 hrs. Enzymatic detection of antigen–antibody interactions was carried out using the Sigma Fast BCIP/NBT system.

Transfection Studies In Vitro

For the immunocytochemical detection of CLIP-115 in COS1 cells, full-length *CLIP-115* (Hi4.8) and δ*CLIP-115* (Hi4.2) cDNAs were excised from λZAP and transfected into COS1 cells. Two days after transfection, the cells were fixed in 100% methanol/1 mM EGTA, blocked in 0.5% BSA/0.02% glycine in PBS, and immunoreacted with antiserum #2131 or #2133 (1:100) and anti-β-tubulin (1:200; Sigma). After washing, sections were incubated with FITC-labeled secondary antibodies (Nordic Laboratories, The Netherlands; 1:80) to detect δCLIP-115 and with rhodamine-labeled sheep anti-mouse (1:20; Boehringer Mannheim) to detect β-tubulin. For direct detection of CLIP-115, three proteins were fused to GFP (Chalfie et al., 1994); these included δCLIP-115, full-length CLIP-115, and CLIP-115$_{1-468}$, a construct that contains a large part of the N-terminal domain with the two MTB domains (upstream of the BssHII site indicated in Figure 2). All constructs were transfected into COS1 cells, and after two days, cells were fixed in 2% paraformaldehyde/PBS and processed for GFP/β-tubulin codetection. To detect CLIP-115 in differentiating neuronal cultures in vitro, hippocampi were dissected from newborn mouse brains, and cells were resuspended and grown on coated glass slides in neurobasal medium (Life Technologies). After 5 days in culture, cells were fixed and processed for immunocytochemistry with #2133 (1:100) and α-MAP2 (1:200; Boehringer Mannheim). Cells were analyzed on an Olympus inverted microscope equipped with GFP/TXR filter blocks, and images were captured with the use of a Sony 3CCD camera (model DXP-950).

Immunocytochemistry In Vivo: Light Microscopy

For analysis of CLIP-115 expression in adult rat brain, Sprague-Dawley rats were anesthetized with sodium pentobarbital (75 mg/kg, intraperitoneally), and perfused with 0.5% zinc salicylate and 4% paraformaldehyde in 0.9% NaCl (pH 5.0). The brains were cryoprotected in saline containing 30% sucrose and cut into 20 μm thick transverse sections on a freezing microtome. All sections were collected in 0.5 M Tris buffer (pH 7.6) with 0.25% Triton-X, blocked in 5% nonfat dry milk in the same buffer for 4 hrs, and incubated for 48 hrs at 4°C with antisera #2131 or #2133 (1:500) or with the affinity-purified antibody (1:20) in 1% nonfat dry milk in 0.5 M Tris buffer with 0.25% Triton. After the primary incubations, sections were rinsed and processed with the use of the avidin–biotin complex method (ABC Elite kit, Vector Laboratories). Finally, the sections were incubated in 0.05% 3,3-diaminobenzidine (DAB) and 0.01% H_2O_2 in 0.05 M Tris buffer, mounted, and coverslipped.

Immunocytochemistry In Vivo: Electron Microscopy

For electron microscopy, adult Sprague-Dawley rats were sacrificed as described above and processed according to published protocols (De Zeeuw et al., 1995). In short, the animals were perfused transcardially, and the brains were sectioned on a Vibratome. These sections were processed for preembedding immunocytochemistry as described above with the use of antisera #2131, #2133, or preimmune sera. Some sections were processed with an antiserum against CLIP-170 (kindly provided by Dr. J. Rickard; for details, see Pierre et al., 1992, 1994; Wacker et al., 1992). Subsequently, sections were osmicated, stained in uranyl acetate, dehydrated in dimethoxypropane, and embedded in Araldite. Guided by semithin sections, we prepared pyramids of the hippocampus and inferior olive. From these tissue blocks, ultrathin sections were cut, counterstained, and examined in a Philips CM 100 electron microscope.

Nocodazole and Taxol Treatment of Olivary Neurons

The effect of microtubule depolymerization on the presence of DLBs was investigated by injecting nocodazole and/or taxol unilaterally into the inferior olive of ketamine anesthetized rats. Prior to the injections, the inferior olive was identified electrophysiologically by the characteristic low firing frequency and waveshape of the action potentials of its neurons (Llinás and Yarom, 1981). Eight adult male Wistar rats received a pressure injection of 5 μg of nocodazole in 20 μl of 25% DMSO through glass micropipettes, two rats received an injection of 1 μg of taxol in 1 μl of DMSO, four rats received both a taxol and nocodazole injection, while four littermates received the drug vehicle only. In the group of eight rats that received only nocodazole, two rats were sacrificed 8 hrs after the injection, two rats after 16 hrs, two rats after 24 hrs, and two rats 48 hrs after the injection. The taxol-treated animals were sacrificed 8 hrs after drug application, while the rats treated with both drugs received taxol 2 hrs prior to nocodazole and were sacrificed 8 hrs later. In all animals, the density of DLBs was investigated immunocytochemically with the use of antiserum α12B/18. Sections were counterstained for cresyl violet, and the neurons were counted and compared to the number of neurons in control animals.

Acknowledgments

We would like to thank Dr. A. Hoogeveen for peptide synthesis and T. Verkerk, R. Hawkins, J. v.d. Burg, M. Kuit, and E. Dalm for their excellent technical assistance. In addition, we thank Dr. J. E. Rickard for kindly providing antisera against CLIP-170. This research was supported by grants from the Netherlands Organization for Scientific Research (NWO; GB-MW 903-68-361), the Life Sciences Foundation (SLW; 805.33.310), and the Royal Dutch Academy of Sciences (KNAW).

Received July 25, 1997; revised October 31, 1997.

References

Allan, V. (1996). Motor proteins: a dynamic duo. Curr. Biol. *6*, 630–633.

Andreasen, M., and Nedergaard, S. (1996). Dendritic electrogenesis in rat hippocampal CA1 pyramidal neurons: functional aspects of Na^+ and Ca^{2+} currents in apical dendrites. Hippocampus *6*, 79–95.

Auffray, C., and Rougeon, F. (1980). Nucleotide sequence of a cloned cDNA corresponding to secreted mu chain of mouse immunoglobulin. Gene *12*, 77–86.

Berlin, V., Styles, C.A., and Fink, G.R. (1990). BIK1, a protein required for microtubule function during mating and mitosis in Saccharomyces cerevisiae, colocalizes with tubulin. J. Cell Biol. *111*, 2573–2586.

Bilbe, G., Delabie, J., Bruggen, J., Richener, H., Asselbergs, F.A., Cerletti, N., Sorg, C., Odink, K., Tarcsay, L., Wiesendanger, W., et al. (1992). Restin: a novel intermediate filament-associated protein highly expressed in the Reed-Sternberg cells of Hodgkin's disease. EMBO J. *11*, 2103–2113.

Burkhardt, J.K. (1996). In search of membrane receptors for microtubule-based motors - is kinectin a kinesin receptor? Trends Cell Biol. *6*, 127–131.

Chalfie, M., Tu, Y., Euskirchen, G., Ward, W.W., and Prasher, D.C. (1994). Green fluorescent protein as a marker for gene expression. Science *263*, 802–805.

Cole, N.B., and Lippincott-Schwartz, J. (1995). Organization of organelles and membrane traffic by microtubules. Curr. Opin. Cell Biol. *7*, 55–64.

Cole, N.B., Sciaky, N., Marotta, A., Song, J., and Lippincott-Schwartz, J. (1996). Golgi dispersal during microtubule disruption: regeneration of Golgi stacks at peripheral endoplasmic reticulum exit sites. Mol. Biol. Cell *7*, 631–650.

Craig, A.M., and Banker, G. (1994). Neuronal polarity. Annu. Rev. Neurosci. *17*, 267–310.

De Zeeuw, C.I., Hertzberg, E.L., and Mugnaini, E. (1995). The dendritic lamellar body: a new neuronal organelle putatively associated with dendrodendritic gap junctions. J. Neurosci. *15*, 1587–1604.

De Zeeuw, C.I., Koekkoek, S.K.E., Wylie, D.R.W., and Simpson, J.I. (1997). Association between dendritic lamellar bodies and complex spike synchrony in the olivocerebellar system. J. Neurophysiol. *77*, 1747–1758.

Feinberg, A.P., and Vogelstein, B. (1983). A technique for radiolabeling DNA restriction endonuclease fragments to high specific activity. Anal. Biochem. *132*, 6–13.

Fourney, R.M., Miyakoshi, J., Day, R.S., and Paterson, M.C. (1988) Northern blotting: efficient RNA staining and transfer. Focus *10*, 5–7.

Gill, S.R., Schroer, T.A., Szilak, I., Steuer, E.R., Sheetz, M.P., and Cleveland, D.W. (1991). Dynactin, a conserved, ubiquitously expressed component of an activator of vesicle motility mediated by cytoplasmic dynein. J. Cell Biol. *115*, 1639–1650.

Hanlon, D.W., Yang, Z., and Goldstein, L.S. (1997). Characterization of KIFC2, a neuronal kinesin superfamily member in mouse. Neuron *18*, 439–451.

Hirokawa, N. (1996). The molecular mechanism of organelle transport along microtubules: the identification and characterization of KIFs (kinesin superfamily proteins). Cell Struct. Funct. *21*, 357–367.

Hofmann, K., and Stoffel, W. (1993). TMbase- a database of membrane spanning proteins segments. Biol. Chem. Hoppe-Seyler *347*, 166.

Holzbaur, E.L., Hammarback, J.A., Paschal, B.M., Kravit, N.G., Pfister, K.K., and Vallee, R.B. (1991). Homology of a 150K cytoplasmic dynein-associated polypeptide with the Drosophila gene Glued. Nature *351*, 579–583. Erratum: Nature *360*(*6405*).

Kolodney, M.S., and Elson, E.L. (1995). Contraction due to microtubule disruption is associated with increased phosphorylation of myosin regulatory light chain. Proc. Natl. Acad. Sci. USA *92*, 10252–10256.

Laird, D.W., Puranam, K.L., and Revel, J.P. (1991). Turnover and phosphorylation dynamics of connexin43 gap junction protein in cultured cardiac myocytes. Biochem. J. *273*, 67–72.

Lewis, S.A., Wang, D.H., and Cowan, N.J. (1988). Microtubule-associated protein MAP2 shares a microtubule binding motif with tau protein. Science *242*, 936–939.

Li, I., Liu, Z.-M., and Nirenberg, M. (1997). Kinesin-73 in the nervous

system of Drosophila embryos. Proc. Natl. Acad. Sci. USA *94*, 1086–1091.

Llinás, R., and Yarom, Y. (1981). Properties and distribution of ionic conductances generating electroresponsiveness of mammalian inferior olivary neurones in vitro. J. Physiol. *315*, 569–584.

Lupas, A. (1996). Coiled coils: new structures and new functions. Trends Biochem. Sci. *21*, 375–382.

Maccioni, R.B., and Cambiazo, V. (1995). Role of microtubule-associated proteins in the control of microtubule assembly. Physiol. Rev. *75*, 835–864.

Matteoni, R., and Kreis, T.E. (1987). Translocation and clustering of endosomes and lysosomes depends on microtubules. J. Cell Biol. *105*, 1253–1265.

Moore, J.D., and Endow, S.A. (1996). Kinesin proteins: a phylum of motors for microtubule-based motility. Bioessays *18*, 207–219.

Ogawa, K., and Mohri, H. (1996). A dynein motor superfamily. Cell Struct. Funct. *21*, 343–349.

Palay, S.L., and Chan-Palay, V. (1974). Cerebellar Cortex: Cytology and Organization (New York: Springer-Verlag).

Pierre, P., Scheel, J., Rickard, J.E., and Kreis, T.E. (1992). CLIP-170 links endocytic vesicles to microtubules. Cell *70*, 887–900.

Pierre, P., Pepperkok, R., and Kreis, T.E. (1994). Molecular characterization of two functional domains of CLIP-170 in vivo. J. Cell Sci. *107*, 1909–1920.

Rickard, J.E., and Kreis, T.E. (1996). CLIPs for organelle-microtubule interactions. Trends Cell Biol. *6*, 178–183.

Saito, N., Okada, Y., Noda, Y., Kinoshita, Y., Kondo, S., and Hirokawa, N. (1997). KIFC2 is a novel neuron-specific C-terminal type kinesin superfamily motor for dendritic transport of multivesicular body-like organelles. Neuron *18*, 425–438.

Sambrook, J., Fritsch, E.F., and Maniatis, T. (1989). Molecular Cloning: A Laboratory Manual, 2nd Ed. (New York: Cold Spring Harbor Laboratory Press).

Schnapp, B.J. (1997). Retroactive motors. Neuron *18*, 523–526.

Sharp, D.J., Yu, W., and Baas, P.W. (1995). Transport of dendritic microtubules establishes their nonuniform polarity orientation. J. Cell Biol. *130*, 93–103.

Smith, P.K., Krohn, R.I., Hermanson, G.T., Mallia, A.K., Gartner, F.H., Provenzano, M.D., Fujimoto, E.K., Goeke, N.M., Olson, B.J., and Klenk, D.C. (1988). Measurement of protein using bicinchoninic acid. Anal. Biochem. *150*, 76–85.

Swaroop, A., Swaroop, M., and Garen, A. (1987). Sequence analysis of the complete cDNA and encoded polypeptide for the Glued gene of Drosophila melanogaster. Proc. Natl. Acad. Sci. USA *84*, 6501–6505.

Takei, K., Stukenbrok, H., Metcalf, A., Mignery, G.A., Sudhof, T.C., Volpe, P., and De Camilli, P. (1992). Ca^{2+} stores in Purkinje neurons: endoplasmic reticulum subcompartments demonstrated by the heterogeneous distribution of the InsP3 receptor, Ca(2+)-ATPase, and calsequestrin. J. Neurosci. *12*, 489–505.

Toyoshima, I., Yu, H., Steuer, E.R., and Sheetz, M.P. (1992). Kinectin, a major kinesin-binding protein on ER. J. Cell Biol. *118*, 1121–1131.

Trueheart, J., Boeke, J.D., and Fink, G.R. (1987). Two genes required for cell fusion during yeast conjugation: evidence for a pheromone-induced surface protein. Mol. Cell. Biol. *7*, 2316–2328.

Vallee, R.B., and Sheetz, M.P. (1996). Targeting of motor proteins. Science *271*, 1539–1544.

Vaughan, K.T., and Vallee, R.B. (1995). Cytoplasmic dynein binds dynactin through a direct interaction between the intermediate chains and p150Glued. J. Cell Biol. *131*, 1507–1516.

Villa, A., Podini, P., Clegg, D.O., Pozzan, T., and Meldolesi, J. (1991). Intracellular Ca^{2+} stores in chicken Purkinje neurons: differential distribution of the low affinity-high capacity Ca^{2+} binding protein, calsequestrin, of Ca^{2+} ATPase and of the ER lumenal protein, Bip. J. Cell Biol. *113*, 779–791.

Wacker, I.U., Rickard, J.E., De Mey, J.R., and Kreis, T.E. (1992). Accumulation of a microtubule-binding protein, pp170, at desmosomal plaques. J. Cell Biol. *117*, 813–824.

Wade, R.H., and Hyman, A.A. (1997). Microtubule structure and dynamics. Curr. Opin. Cell Biol. *9*, 12–17.

Watanabe, T.K., Shimizu, F., Nagata, M., Kawai, A., Fujiwara, T., Nakamura, Y., Takahashi, E., and Hirai, Y. (1996). Cloning, expression, and mapping of CKAPI, which encodes a putative cytoskeleton-associated protein containing a CAP-GLY domain. Cytogenet. Cell Genet. *72*, 208–211.

Waterman-Storer, C.M., Karki, S., and Holzbaur, E.L. (1995). The p150Glued component of the dynactin complex binds to both microtubules and the actin-related protein centractin (Arp-1). Proc. Natl. Acad. Sci. USA *92*, 1634–1638.

Yamashita, A., Watanabe, Y., and Yamamoto, M. (1997). Microtubule-associated coiled-coil protein Ssm4 is involved in the meiotic development in fission yeast. Genes Cells *2*, 155–166.

GenBank Accession Number

The EMBL accession number of the *CLIP-115* cDNA sequence is AJ000485.